Dielectron physics with ALICE Transition Radiation Detector

Prashant Shukla (for the ALICE TRD Collaboration)

Physikalisches Institut der Universität Heidelberg, Philosophenweg 12, 69120 Heidelberg, Germany

E-mail: shukla@physi.uni-heidelberg.de

Abstract. The Transition Radiation Detector (TRD) of ALICE will serve to identify and track electrons in the central region. In this contribution, after a brief introduction of TRD, we review the detector performance concerning electron/pion identification as well as J/ψ and Υ detection.

.

1. Introduction

The ALICE experiment will study the collision process of lead nuclei at a center of mass energy per nucleon pair of 5.5 TeV at the CERN Large Hadron Collider (LHC). These collisions will create very high energy density well above the estimated threshold of forming Quark Gluon Plasma (QGP). One of the most interesting probes of QGP are heavy vector resonances $J/\Psi, \Psi^{'}, \Upsilon, \Upsilon^{'}, \Upsilon^{''}$ through their leptonic decays. The complexity of heavy quark physics at LHC energies calls for comprehensive measurements of heavy quark and quarkonia production in pp, pA and AA collisions. The Transition Radiation Detector (TRD) [1, 2] of ALICE is placed in the Central Barrel. Via the dielectron channel, the production of light and heavy vector mesons as well as the continuum will be measured. The single electron channel will measure the semi-leptonic decays of hadrons with open charm (D) and open beauty (B) using the displaced vertex information provided by the ITS. The correlated production of $D\bar{D}$ and $B\bar{B}$ can be studied via coincidences of electrons in the central barrel and muons in the forward muon arm. The task of TRD is to identify electrons from the dominant background of pions. In addition, it will serve as a trigger for electrons with momenta higher than 2 GeV/c.

2. Transition Radiation Detector

The TRD is placed between Time Projection Chamber(TPC) and Time of Flight (TOF) and covers a pseudorapidity range $|\eta| \leq 0.9$. The TRD is segmented into 18 sectors in azimuth, each subdivided into 5 sections along the beam axis and six layers of chambers in the radial direction. This adds up to 540 detector modules. The largest chamber dimension is 120 x 159 cm^2. A schematic view of a detector module and its principle is shown in Fig.1. Each module comprises a radiator (4.8 cm, fiber/foam) followed by an ionization and drift gap (3 cm) and a multiwire proportional counter (0.7 cm) filled with Xe/CO_2(85:15). When an electron passes through the radiator it generates Transition Radiation (TR). The electron while traversing the gas produces

ionization as do pions. Both the ionization electrons and those from the absorption of the TR photons drift towards the amplification region and produce avalanches around anode wires, which induces signal on the cathode pads. The pad signals are sampled in 20 time bins.

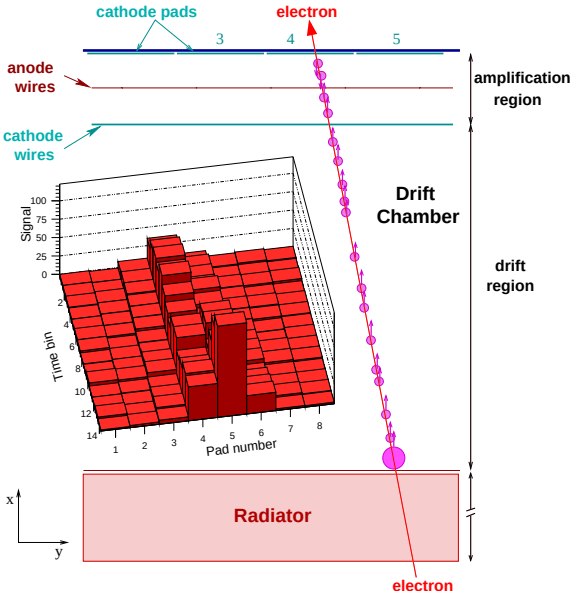

Figure 1. TRD module and its principle.

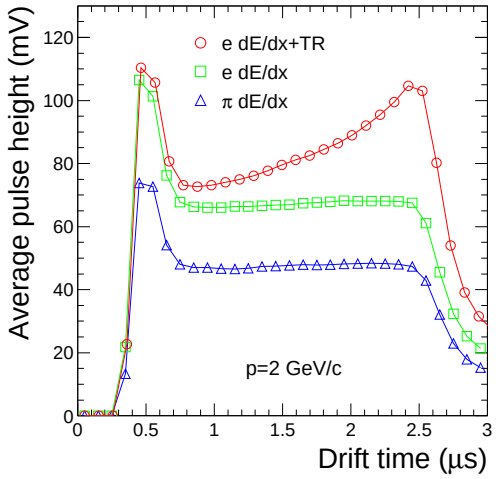

Figure 2. A pulse height spectrum from TRD module.

Figure 2 shows average pulse height distributions measured in the TRD chamber as a function of drift time. The peak at early drift times is generated by the charge deposited in the amplification region. While the pion spectrum is rather flat at larger drift times, the electron spectrum is peaked at late times since larger energy is deposited towards longer drift times corresponding to TR photons absorbed predominantly at the entrance of the chamber.

An online trigger is required to tag events, with high p_t electrons. The 20 time samples of the ADC are fed into a digital chip for zero suppression, gain calibration and tail cancellation of the signal. The data are subsequently processed by the local tracking unit (LTU) on the same chip, which calculates the hit position in each time bin and builds local tracklets. An electron likelihood factor based on integrated charge is associated to each tracklet. The information from the different LTUs is subsequently fed into the global tracking unit (GTU). The GTU associates tracklets to tracks and fits the track parameters and applies a cut in the transverse momentum. The track electron likelihood function is derived from the tracklet likelihood information. The performance of this online trigger was extensively studied in simulations [2].

3. Electron/pion identification

The pion efficiency is calculated for different electron efficiencies by the likelihood method using measured data. The required pion rejection factor for quarkonia measurement should be 100 at 90 % electron efficiency. Figure 3 shows the measured and simulated pion efficiency as a function of number of layers. The performance of six layers fulfills the requirement on pion rejection.

Figure 4 shows the pion efficiency as a function of momentum. The filled triangles (L_Q) are obtained by likelihood on measured integrated charge. The hollow triangles are simulations where the foam/fiber radiator is modelled by a stack of variable number of foils. Filled circles are obtained by bidimensional likelihood (L_{QX}), for which the distribution of the time bin of the maximum amplitude is used together with the integrated charge [3]. An improvement of the

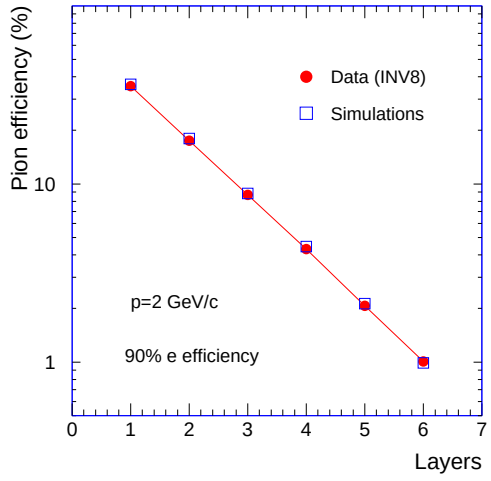

Figure 3. Pion efficiency as a function of number of layers.

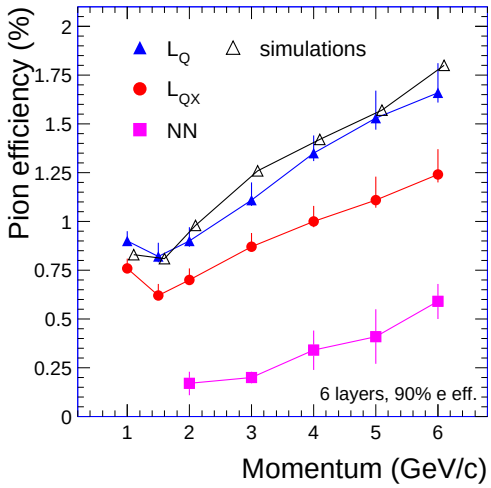

Figure 4. Pion efficiency as a function of momentum.

pion rejection by a factor up to 1.3 is achieved with this method. Solid squares are obtained with a neural network (NN) approach which further improves the pion rejection factor up to 4.5 times. The results presented above are for the ideal case of isolated tracks. However, for real events in ALICE a degradation of the performance is expected as a function of multiplicity [2].

4. Quarkonia signal $J/\Psi, \Upsilon$

The position resolution from one TRD chamber is about 400 μm in ϕ-direction. The combined ITS-TPC-TRD momentum resolution dp_t/p_t at $p_t = 1$ GeV/c and 5 GeV/c has been shown to be 1% and 1.8 %, respectively [4]. Figure 5 shows a dielectron invariant mass simulation with AliRoot [5]. Charged pions are generated with a parameterized HIJING model for a rapidity density dN/dy = 2000. The signals in the dielectron channel amount to 0.03 J/Ψ and $4{\times}10^{-4}$ Υ. The combinatorial background is due to the semielectronic deacys from 115 $c\bar{c}$ and 5 $b\bar{b}$ included per event. The solid line is derived by TPC information only, which contains substantial amount of misidentified pions. The dashed line includes TRD which reduces the combinatorial background by more than an order of magnitude.

The signal to background ratio, S/B as function of a single track p_t-cut is shown in Fig. 6. The background from semileptonic decays of D and B mesons as well as misidentified pions are concentrated at lower transverse momentum p_t. The S/B can therefore be optimized by a judicious choice of such a cut. Here, the two curves TPC2 and TPC3 represent two different pion efficiencies based on different assumed TPC pion rejection. The combined TRD-TPC mass resolution for J/Ψ and Υ is about $\sigma^M_{J/\Psi} \sim 27$ MeV/c^2 and $\sigma^M_{\Upsilon} \sim 75$ MeV/c^2, respectively. These values indicate the Υ-family to be well resolved.

5. Conclusions

The ALICE TRD is well suited to study quarkonia production in the high multiplicity environment of Pb+Pb collisions at LHC. Test measurements have shown that the required electron/pion separation can be achieved. At the trigger level, rare heavy mesons like Υ can be selected. In conjunction with other detectors in the central barrel, the signal from the Υ family

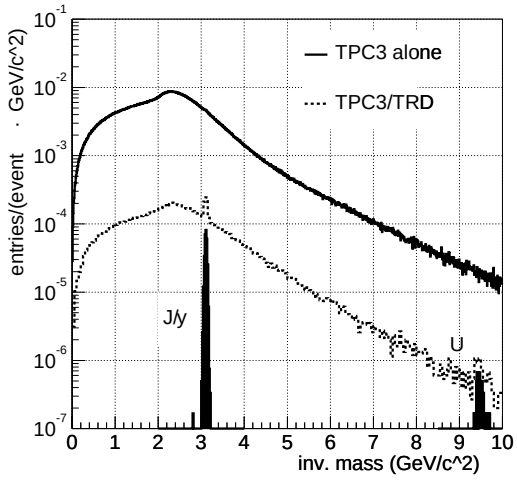

Figure 5. Dielectron mass spectrum.

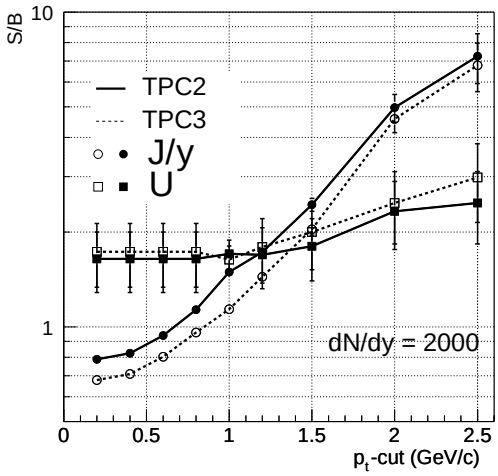

Figure 6. The signal to background ratio.

can be observed with a mass resolution of 1 %.

ALICE TRD Collaboration

C. Adler[1], A. Andronic[2], V. Angelov[3], H. Appelshäuser[4], S. Bablok[11], C. Baumann[5], R. Bailhache[2], C. Blume[4], P. Braun-Munzinger[2], D. Bucher[5], O. Busch[2], V. Cătănescu[1,6], V. Chepurnov[7], S. Chernenko[7], P. Christakoglou[9], E.S. Conner[11], H. Daues[2], J. de Cuveland[3], D. Emschermann[1], O. Fateev[7], Y. Foka[2], S. Freuen[1], C. Garabatos[2], R. Glasow[5], D. Gottschalk[3], H. Gottschlag[5], J.F. Grosse-Oetringhaus[5], T. Gunji[8], M. Gutfleisch[3], H. Hamagaki[8], G. Hartung[10], J. Hehner[2], N. Heine[5], N. Herrmann[1], H. Höbbel[3], M. Hoppe[5], U. Kebschull[3], R. Keidel[11], E. Kislov[7], V. Kiworra[3], C. Klein-Bösing[5], E. Kofler[11], T. Krawutschke[10], V. Lindenstruth[3], C. Lippmann[2], T. Mahmoud[1], P. Malzacher[2], A. Marin[2], J. Mercado[1], D. Miskowiec[2], Y. Morino[8], K. Oyama[1], Yu. Panebratsev[7], V. Petracek[1], A. Petridis[9], M. Petrovici[6], S. Radomski[2], A. Radu[2,6], C. Reichling[3], K. Reygers[5], I. Rusanov[1], S. Saito[8], A. Sandoval[2], R. Santo[5], R. Schicker[1], R. Schneider[3], K. Schwartz[2], P. Shukla[1], R.S. Simon[2], L. Smykov[7], H.K. Soltveit[1], W. Sommer[4], J. Stachel[1], H. Stelzer[2], M.R. Stockmeier[1], G. Stoicea[6], H. Tilsner[3], G. Tsiledakis[2], M. Vassiliou[9], W. Verhoeven[5], B. Vulpescu[1], J.P. Wessels[5], A. Wilk[5], B. Windelband[1], Yu. Zanevsky[7], V. Yurevich[7].

[1]PI Universität Heidelberg, Germany, [2]GSI Darmstadt, Germany, [3]KIP Heidelberg, Germany, [4]IKF Universität Frankfurt am Main, Germany, [5]IKP Universität Münster, Germany, [6]NIPNE Bucharest, Romania, [7]JINR Dubna, Russia, [8]University of Tokyo, Japan, [9]University of Athens, Greece, [10]Fachhochschule Köln, Germany, [11]Fachhochschule Worms, Germany.

References

[1] ALICE Collaboration 1999 *A Transition Radiation Detector, Technical Proposal* Addendum 2, CERN/LHCC/1999-13

[2] ALICE Collaboration 2001 *Transition Radiation Detector, Technical Design Report* CERN/LHCC/2001-021

[3] Andronic A et al. 2004 *Nucl. Instr. Meth.* A **522** 40 (*Preprint* physics/0402131)

[4] Safarik K 2005 *Nucl. Phys. A* **749** 229

[5] Mahmoud T 2004 *Doctoral thesis: Development of readout chamber of the ALICE Transition Detector and Evaluation of its Physics Performance* (University of Heidelberg)